Progress In Electromagnetics Research C, Vol. 102, 163–174, 2020

High Permittivity Substrate and DGS Technique for Dual-Band Star-Shape Slotted Microstrip Patch Antenna Miniaturization

Zhor Bendahmane*, Souheyla Ferouani, and Choukria Sayah

Abstract—Three miniaturization techniques were combined in this work to achieve compact size while maintaining optimal performances of a dual-band star shape slotted Microstrip Patch Antenna (MPA) operating at 2.4 and 5 GHz resonant frequencies. High permittivity substrate and slot techniques were used for miniaturization and impedance matching improvement, while DGS technique was necessary for bandwidth enhancement and further miniaturization of the reference MPA. The miniaturized antenna shows a planar structure and occupies a very small area of $15.55 \times 19.80\,\text{mm}^2$ achieving patch size area reduction of 71.24% and overall size reduction of 75.42%. Respectable positive gains were maintained with radiation efficiency exceeding 83% and 68% at 2.4 GHz and 5 GHz, respectively. The reference and miniaturized MPAs were fabricated, then their performances were measured and compared to the simulated ones. The measured impedance bandwidths of the miniaturized MPA were around 38% and 13% at the two resonant frequencies, respectively, which confirm the originality and suitability of the miniaturized MPA for Wireless Local Area Network WLAN and ISM applications.

1. INTRODUCTION

Owing to the significant emphasis in current research on realization of compact wireless multifunctional devices, design methods have been hinged on efficiently modifying and optimizing the antenna shape and overall geometry, to have sufficient area and volume with desirable operating characteristics.

The concept of antenna miniaturization is to reduce the size of these proven systems while maintaining, to a reasonable degree, the performances of the original antenna in terms of gain, bandwidth, impedance matching, and efficiency, although this is a difficult and daunting task [1]. The most prominent antenna miniaturization techniques can be divided into two main categories: topology and material-based methods. Each category consists of several different classes, including antennas based on space-filling curves, fractals, meander lines, engineered ground planes, reactive loads, slow-wave structures, meta-materials, and high dielectric constant material [2].

One efficient way to reduce the antenna size is by keeping the physical size intact while slowing the wave propagation and consequently decreasing the guided wavelength using a material with high dielectric constant. This approach is most suitable for Microstrip Patch Antennas, in which a higher dielectric constant for the substrate results in a lower resonant frequency for its dominant mode. Based on this relationship between size and electromagnetic properties of the substrate, several MPA miniaturization works have been developed utilizing substrates with high dielectric constant material [3–5].

Surface-wave loss and narrow bandwidth were two undesirable effects brought back by the use of a high permittivity substrate, so to mitigate this surface-waves and enhance the antenna bandwidth, and other techniques are combined to this technique such as meander [6] or spiral slots [7], and Defected Ground Structure (DGS), which consist of periodic or aperiodic geometric defects etched on the ground

Received 15 February 2020, Accepted 9 April 2020, Scheduled 27 May 2020
* Corresponding author: Zhor Bendahmane (zh_bendahmane@yahoo.fr).
The authors are with the Smart Structures Laboratory, Ain Temouchent University, Algeria.

of planar antennas disturbing its shield current distribution and consequently improving the antenna performances.

Often the ground plane acts on the performance of miniaturized MPAs since the size reduction of the radiating element correspondingly affects the dimensions of the ground plane. It is the reason that DGS technique has become one of the most interesting ways to overcome the limitation of a compact antenna, in terms of gain [8], Cross-Polarized Radiation [9, 10], and impedance bandwidth [11, 12].

The main prospect of this work is to investigate reconfigurable properties of the proposed compact antenna, since the motivation for implementing reconfigurable properties in an antenna is the acquisition of new capabilities, which exclude the need for multiple antennas and/or offer additional degrees of operational autonomy that expand system performances.

The concept of reconfigurable printed antenna suggests its ability to dynamically adapt one or more of its fundamental characteristics such as frequency (central frequency, bandwidth), polarization (type of polarization, orientation), and radiation pattern (beamwidth and direction, shape of the pattern) by using reconfiguration techniques which are divided into four major categories: electrical, optical, mechanical, and material change [13].

Electrical reconfiguration techniques are based on active components (MEMS-RF, Diode PIN, Varactor) that are able to change their base characteristics and which are directly integrated with the antenna: using surface PiN diodes for Silicon-based antenna [14], or mounted on the antenna: [15, 16] using PiN diodes for achieving frequency reconfigurability. The electrical reconfiguration technique has gained popularity among all the techniques reported for their low cost, ease of integration, and the versatility of antennas using this technique of reconfiguration.

This paper provides an analysis of interest of high permittivity and thin substrate for the miniaturization of a dual-band star-shape slotted MPA designed and optimized for satisfying WLAN-IEEE-802.11 and ISM bands. The alteration of the central star slot and the addition of DGS result in better impedance matching, wider impedance bandwidth, and acceptable positive gain with improved efficiency for WI-FI and ISM applications.

The rest of the paper is structured as follows. Section 2 presents the miniaturized antenna design details. Section 3 presents simulated and measured results interpretation, and Section 4 concludes the paper.

2. MINIATURIZED ANTENNA DESIGN AND INVESTIGATION

First of all, the reference patch antenna consists of a rectangular star shape slotted MPA with patch dimensions of $28.5 \times 37.56\,\text{mm}^2$, printed on an FR-4 substrate, having permittivity $\varepsilon_r = 4.3$, thickness $h = 1.5\,\text{mm}$, and dielectric loss tangent of 0.025. A microstrip feed line placed on the top layer of the substrate is used for providing $50\,\Omega$ input impedance to the patch, while a total ground plane is placed on the bottom layer covering the complete structure.

This reference antenna already proposed in [17] has been designed to operate at 2.4 and 5 GHz resonant frequencies and is considered as the basis for the comparison in terms of size reduction. Three design steps are necessary for the antenna miniaturization while the fourth step aims to bandwidth enhancement of the antenna.

2.1. Step 1: Utilization of High Permittivity Substrate

The miniaturization strategy starts by keeping the same geometry and dimensions of the reference MPA structure, and only the FR-4 substrate has been changed to a relatively high dielectric constant substrate which is Rogers RT 6010, having permittivity $\varepsilon_r = 10.2$, thickness $h = 1.27\,\text{mm}$, and dielectric loss tangent of 0.0023. Figure 1 depicts the reference antenna shape, while Table 1 shows the optimized dimensions of the antenna.

The return loss (S_{11}) variation of the reference MPA on FR4 and Rogers RT6010 substrates are both plotted in Figure 2.

As indicated in Figure 2, the first dominant mode or the lower resonant frequency f_l of the reference MPA has shifted to lower frequency region by using RT6010 having higher permittivity than that of FR4 substrate. The RT6010 MPA resonates at 1.61 GHz instead of 2.42 GHz for the FR4 antenna.

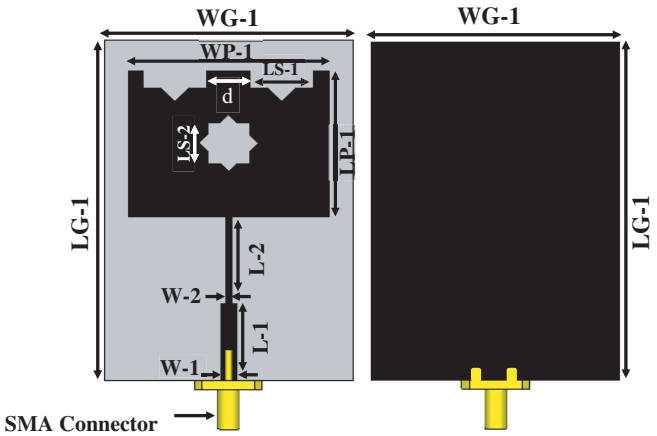

Figure 1. Reference FR-4 dual-band MPA structure.

Table 1. Dimensions of the reference patch antenna.

Parameters	Value (mm)	Parameters	Value (mm)
LP-1	28.50	W-1	2.98
WP-1	37.56	W-2	1.10
LG-1	66.60	LS-1	10.00
WG-1	46.56	LS-2	7.50
L-1	15.00	d	12.00
L-2	17.10	h	1.5

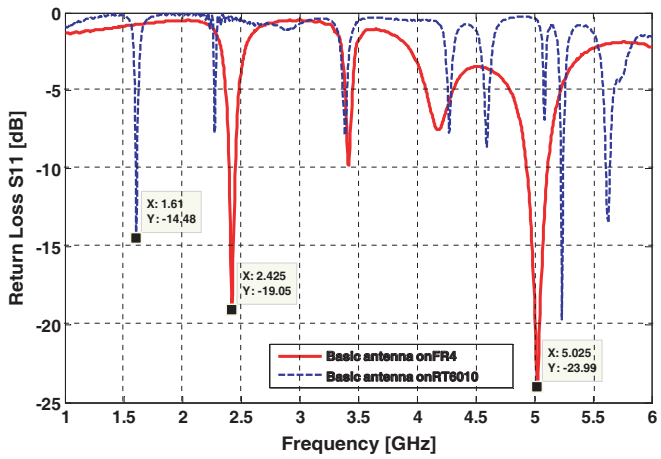

Figure 2. Return loss for the FR4 and RT6010 conventional antenna.

2.2. Step 2: Miniaturization Process

Trying to regain previous resonant frequencies it is necessary to decrease the size of the patch. Indeed, the antenna size is inversely proportional to the dielectric constant ε_r of the substrate Eq. (1), [18]

$$L = \frac{\lambda_g}{2} = \frac{\lambda_0}{2\sqrt{\varepsilon_{eff}}} = \frac{C}{2f_l\sqrt{\varepsilon_{eff}}} \quad (1)$$

where L is the side length of the rectangular patch, λ_g the guided wavelength dependent on the substrate dielectric ε_r, λ_0 the free space wavelength, C the velocity of light in free space, and ε_{eff} the effective permittivity.

Therefore, starting by reducing the length and width (LP-1 and WP-1) of the RT6010 radiating element to recovering the FR4 reference antenna performances (S_{11}, bandwidth, gain ...), the other dimensions of the antenna must be decreased accordingly. Figure 3 shows the return loss variation of the antenna, and Table 2 marks the first and second −10 dB return losses for several (LP-1 and WP-1) values.

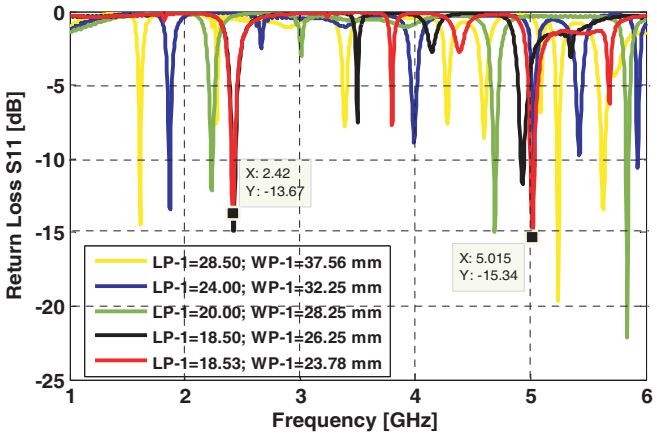

Figure 3. Return loss of antenna by varying LP-1 and WP-1 parameters.

Table 2. Effect of patch dimensions on the antenna resonance.

LP-1 (mm)	WP-1 (mm)	First resonance (GHz)	Second resonance (GHz)
28.50	37.26	1.61	5.24
24.00	32.25	1.87	5.93
20.00	28.25	2.24	4.69
18.50	26.25	2.42	4.93
18.53	23.78	2.42	5.02

It is clear from Figure 3 and Table 2 that by decreasing the dimensions of the antenna its resonant frequencies have remarkably shifted to high frequency; thereby, the reference antenna resonance frequencies were reached for LP-1 = 18.53 mm and WP1 = 23.78 mm, but the level of impedance matching remained relatively low, −13.68 dB at 2.42 GHz and −15.34 dB at 5.015 GHz frequency.

2.3. Step 3: Slot Shape Alteration

In order to improve the size reduction and impedance matching of the miniaturized antenna, the centered star slot has been changed to a ring star slot shape as shown in Figure 4.

Parametric study simulations have been performed on the ring-star slot width WS as shown in Figure 5, and then dimensions of the miniaturized antenna have been optimized to regain reference antenna performances in terms of resonance frequencies and impedance matching as displayed in Table 3.

According to Figure 5 and Table 3, the parameter value (WS = 0.7 mm) allows better impedance matching for the miniaturized antenna except that its bandwidths have decreased and are not sufficient for WLAN applications, 32.4 MHz of bandwidth at 2.4 GHz resonant frequency, and 35.9 MHz at 5 GHz. It should be noted that up to this step of the miniaturization process the antenna has a total ground plane.

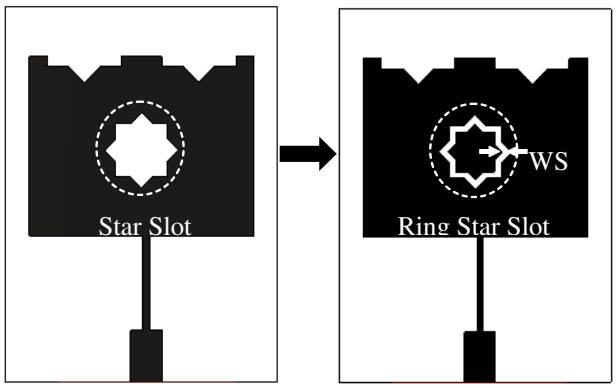

Figure 4. Centered star slot shape modification.

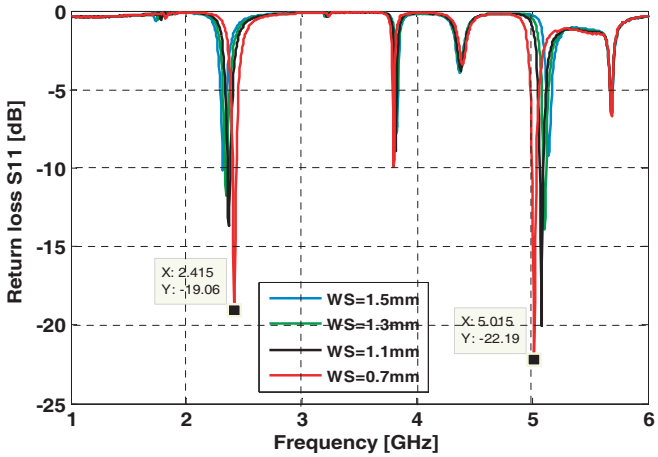

Figure 5. Return loss of antenna by varying star slot width WS.

Table 3. Effect of ring star slot width WS on the antenna impedance matching.

WS (mm)	Low resonance (GHz)	S_{11} (dB)	High resonance (GHz)	S_{11} (dB)
1.5	2.32	−10.14	5.14	−9.23
1.3	2.35	−11.75	5.11	−13.89
1.1	2.37	−13.71	5.08	−20.04
0.7	2.42	−19.06	5.02	−22.19

2.4. Step 4: DGS for Miniaturized MPA Bandwidth Enhancement

This design step not only is used for the antenna bandwidth enhancement at its two resonant frequencies, but also improves the antenna miniaturization. By reducing patch dimensions, the ground plane and substrate are necessarily abridged and result in space diffraction and surface waves over extremities of the ground plane owing to the finite nature of its lateral dimensions; this is the reason to engrave compact geometric pattern defects at these locations, and for our design, we decide to use the simplest shape of slots to model and study, which is the rectangular shape.

Figure 6 shows the ground surface current distribution at the lowest and highest resonant frequencies of the miniaturized antenna.

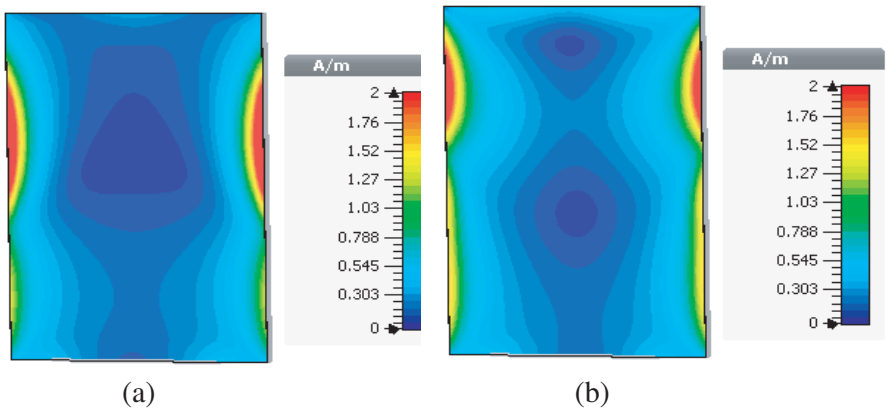

Figure 6. Surface current distribution at (a) 2.4 GHz; (b) 5 GHz.

It can be seen that the surface current is more intense at the right and left sides of the ground plane for the two resonant frequencies. Figure 7 shows DGS configurations evolution investigated to augment antenna bandwidth. Figure 8 illustrates the return loss S (11) for four configurations, and Table 4 summarizes the effect of different configurations on the resonant frequencies and the bandwidths of the proposed antenna.

According to Figure 8 and Table 4, it can be noticed that the three DGS configurations, Case 1, Case 2, and Case 3, have introduced the third intermediate resonance with impedance matching less

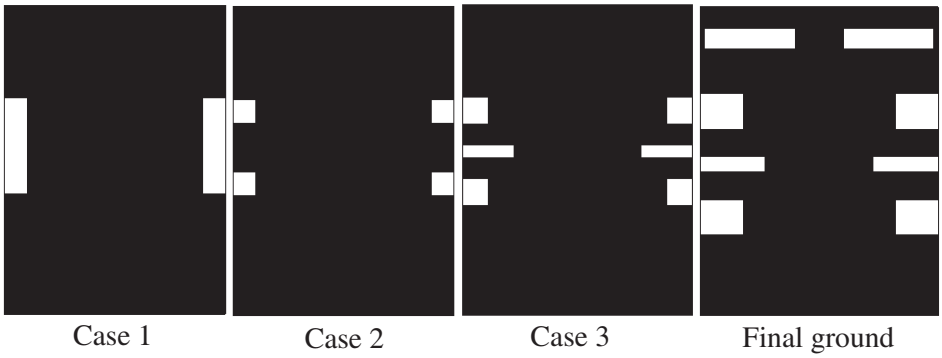

Figure 7. DGS configurations progression.

Table 4. Effect of DGS configurations on the antenna resonance frequencies and bandwidths.

DGS Configurations	**First Resonance Frequency f1 [GHz]**	**Second Resonance Frequency f2 [GHz]**	**Third Resonance Frequency f3 [GHz]**	**Bandwidths [MHz]**
Case 1	2.38	3.83	5.02	38, 11, 36
Case 2	2.39	3.81	5.04	43, 12, 14
Case 3	2.36	4.63	5.1	76, 41, 28
Final Configuration	2.42	-	5	109, 57

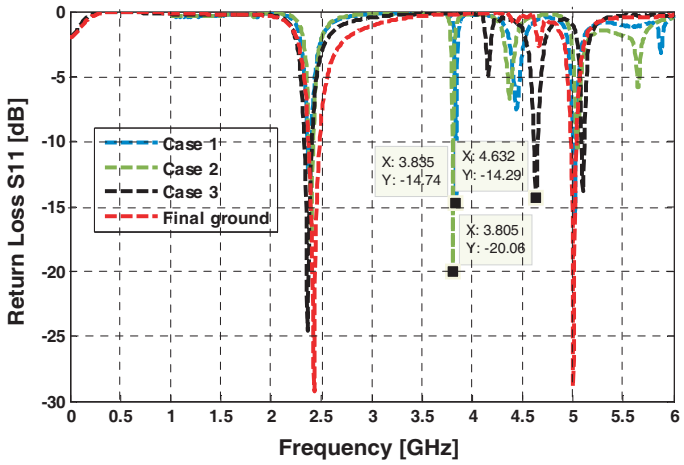

Figure 8. Return loss for different DGS configuration.

than −10 dB, which is not the aim of this study, then by adding the two upper slots, final ground configuration, the intermediate resonance has been removed, and the impedance matching for the two useful bands of the proposed MPA has been improved.

For the proposed design, there is symmetry for the six slots positioned on the right and left lower-lateral parts of the ground plane, which allowed a widening of the bandwidth at the two resonant frequencies but introduced new resonances to the proposed MPA. The positions, dimensions, and number of slots have been the subject of several parametric studies.

Afterward, parametric studies have been performed to fix the number, dimensions, as well as the positions of the upper slots, which remove the intermediate resonances, then all the eight slots' dimensions have been optimized in terms of return loss, to find the widest bandwidths for our antenna.

At the end of this design progression, the antenna dimensions have been optimized using CST software based on the Finite Integration Technique (FIT) to obtain the best impedance matching and bandwidths at the two resonant frequencies. Figure 9 depicts the miniaturized antenna shape, while Table 5 shows the antenna dimensions.

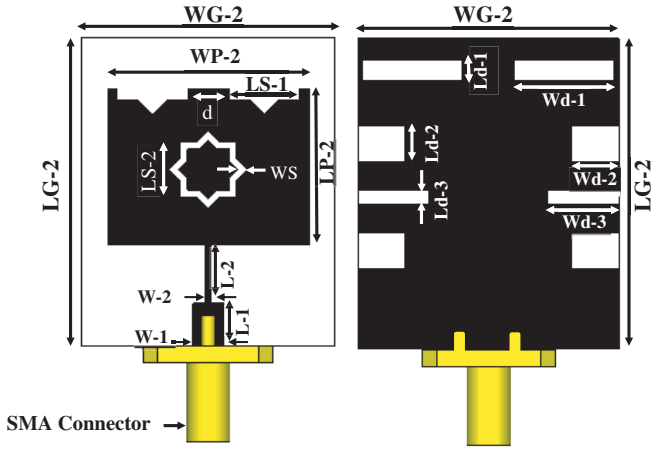

Figure 9. Miniaturized RT-6010 dual-band MPA geometry.

3. SIMULATED AND MEASURED RESULTS INTERPRETATION

Before going towards the fabrication of conventional and miniaturized antennas, their dimensions were optimized, and mesh adaptation was performed using high-frequency simulator software to obtain

Table 5. Detailed dimensions of the miniaturized antenna.

Parameters	Value (mm)	Parameters	Value (mm)	Parameters	Value (mm)
LP-2	15.55	WS	0.70	W-1	3.00
WP-2	19.80	d	4.00	W-2	0.56
LG-2	30.63	Wd-1	9.50	LS-1	7.00
WG-2	24.88	Ld-1	2.00	LS-2	5.50
L-1	4.20	Wd-2	4.50	Wd-3	6.80
L-2	5.80	Ld-2	3.50	Ld-3	1.50
h	1.27	-	-	-	-

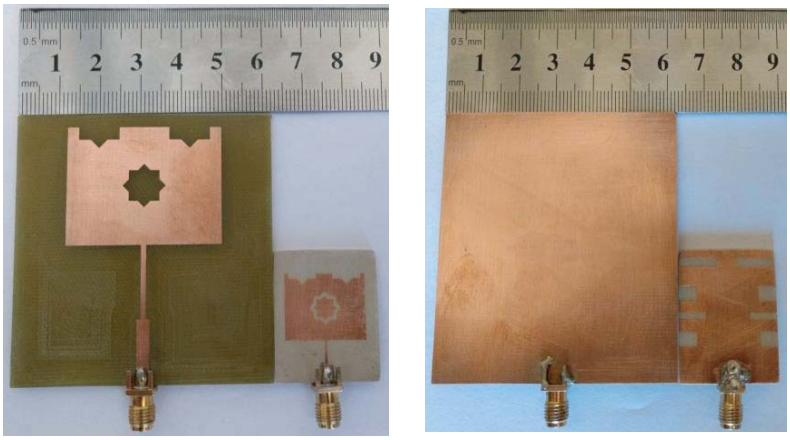

(a) (b)

Figure 10. Photographs of conventional and miniaturized MPA: (a) Top view, (b) bottom view; parameters as in Tables 1 and 5.

concordance between the measured and simulated performances. The representative photographs of both reference and miniaturized MPA prototypes are shown in Figure 10.

3.1. Return Loss S_{11} and Bandwidth Performances

The S_{11} characteristics of the reference and miniaturized MPAs are measured via the Anritsu MS2028C vector network analyzer with a range of 5 KHz to 20 GHz, and represented with the simulated ones as a function of frequency in Figures 11 and 12.

The simulated return loss of reference MPA shows a dual-band behavior at 2.42 GHz and 5.03 GHz with good impedance matching S_{11} less than -19.35 dB and -23.57 dB, and fractional bandwidth (FBW) exceeding 22% from 2.39 GHz to 2.45 GHz and 35% from 4.93 GHz to 5.11 GHz at the two frequencies, respectively, which is confirmed by the measurement results offering S_{11} less than -20.26 dB and -17.73 dB with FBW exceeding 79% from 2.44 GHz to 2.62 GHz and 25.5% from 5.06 GHz to 5.19 GHz at 2.47 GHz and 5.13 GHz, respectively.

The simulated return loss of the miniaturized MPA has kept dual-band characteristic at 2.42 GHz and 5 GHz with respective impedance matching less than -29 dB and -28 dB and FBWs about 45% from 2.37 GHz to 2.48 GHz and 12% from 4.97 GHz to 5.03 GHz. The measured results have confirmed the simulation with S_{11}, less than -37.04 dB and -19.06 dB and FBWs exceeding 38% to suppress and 13% at 2.46 GHz and 5.11 GHz, respectively.

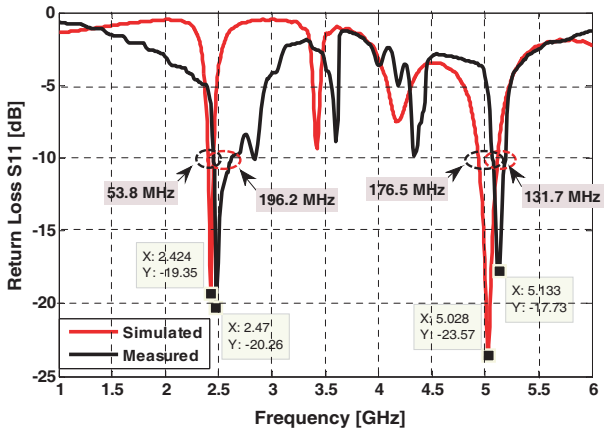

Figure 11. Simulated and measured return loss of reference FR4 antenna.

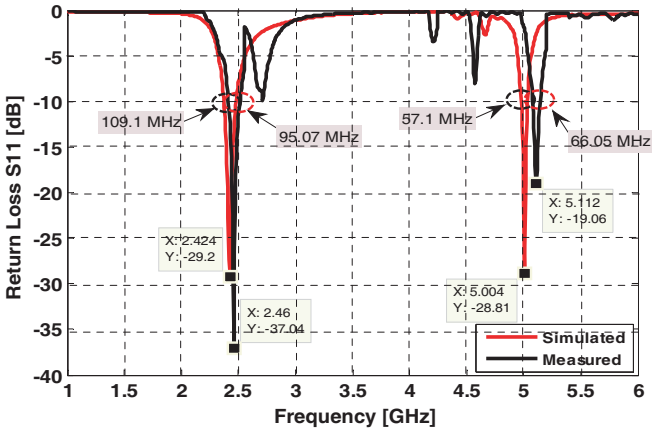

Figure 12. Simulated and measured return loss of the miniaturized antenna.

3.2. Radiation, Gain and Efficiency Characteristics

The miniaturized and reference MPA E-plane and H-plane radiation performances are plotted in Figure 13 at 2.4 GHz and 5 GHz.

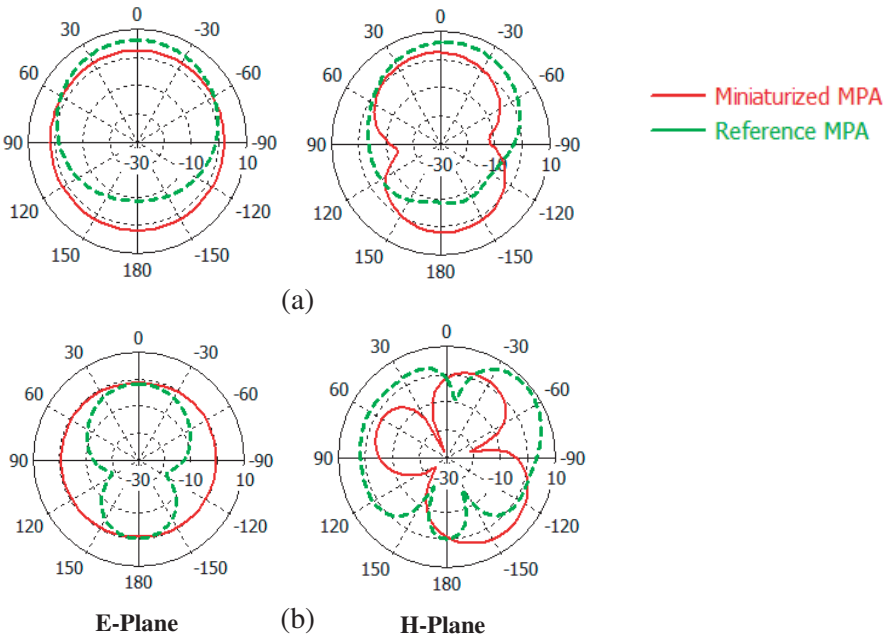

Figure 13. Miniaturized and Reference MPA radiation patterns in E-plane and H-plane at (a) 2.4, and (b) 5 GHz.

The radiation patterns reveal almost omnidirectional and stable radiation patterns at both frequencies 2.4 GHz and 5 GHz for the reference and miniature antennas.

It is also observed that there is an expansion of the miniaturized radiation patterns compared to those of the reference antenna proving the effect of the increase in substrate permittivity on widening and coherence maintain of the radiation diagram [18].

As marked in Figure 14, the reference antenna achieves gain surpassing 6 dBi and 8 dBi with efficiency not above 60% at the two resonant frequencies, respectively.

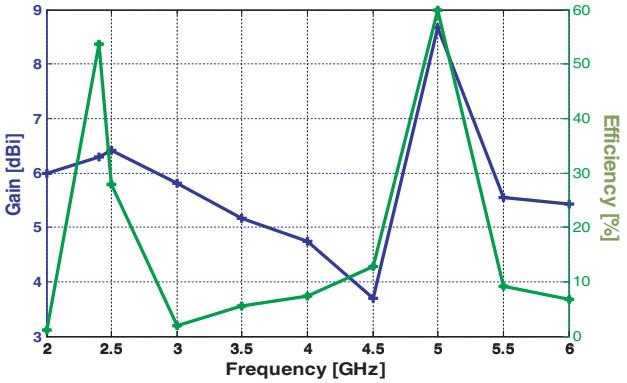

Figure 14. Reference MPA gain and efficiency.

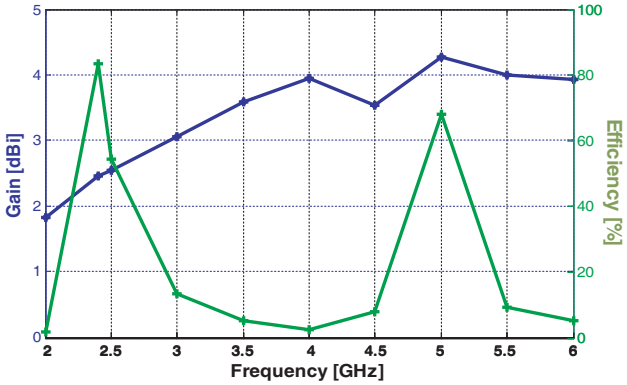

Figure 15. Miniaturized MPA gain and efficiency.

The miniaturized MPA assures better efficiency than the reference MPA exceeding 83% and 68% with gain above 2.45 dBi and 4.27 dBi at resonant frequencies 2.4 GHz and 5 GHz, respectively, as illustrated in Figure 15.

3.3. Comparison and Discussion

To contrast and distinct the performances of the miniaturized MPA proposed in this paper, a comparison with some recent related works from literature is summarized in Table 6.

Table 6. Comparison of the proposed miniaturized antenna with other antennas from literature.

Reference	Frequency band (GHz)		Miniaturization Ratio	−10 dB Fractional Bandwidth (%)		Maximum Gain (dBi)		Efficiency (%)	
	Band 1	Band 2		Band 1	Band 2	Band 1	Band 2	Band 1	Band 2
[19]	2.43	5.2	74%	1.6	23.08	−1.7	2.4	30	81
[20]	1.9	3.5	38%	4	2.2	1	2.4	28	35
[21]	2.36	8.45	89%	24	10.36	−1.25	2.8	-	-
[22]	2.2	2.68	50%	45.90	5.45	6.26	3.59	90	82
[23]	2.4	5.5	$0.28\lambda \times 0.24\lambda$	10	6	1	0.26	78	75
[24]	3.17	5.39	$0.23\lambda \times 0.21\lambda$	2.89	3.71	0.71	1.89	66	85
[25]	3.52	5.17	$0.20\lambda \times 0.14\lambda$	11.53	5.95	1.44	2.70	90.90	97.30
[11]	3.53	6.83	$0.40\lambda \times 0.40\lambda$	12.49	4.49	4.02	3.38	88.20	76.88
This Work	**2.46**	**5.11**	**71%** $\mathbf{0.24\lambda \times 0.20\lambda}$	**38**	**13**	**2.45**	**4.27**	**83**	**68**

The authors in [19, 21, 25] have reported better miniaturization rates than that of the proposed antenna, by using shorting post with DGS, U-shaped transmission lines, and meander with stub techniques respectively; however, their fractional bandwidth and gain remain feeble compared to those of the proposed MPA. Also the antennas proposed in [19] and [21] show negative gain at their low resonant frequency which affects their overall MPA's performances. In [21], metamaterial superstrate having large dimensions was used for gain improvement, increasing thereby the antenna volume.

The other reported contributions in [11, 20, 22–24] indicate lower performances in terms of FBW and gain except the antenna proposed in [22] which exhibits superior FBW and gain at its lower resonant frequency compared to that of the proposed MPA, and even if efficiencies of some reported works such

as [22] and [25] are more important to those of the proposed MPA, their miniaturization rate stays weak which explains these performances.

For the proposed design, significant miniaturization rate is achieved by using high permittivity substrate combined to DGS technique which made it possible to widen the bandwidths of the antenna while keeping appreciable positive gains and good efficiencies at both resonance bands.

4. CONCLUSION AND FUTURE WORK

High permittivity substrate technique is combined to slot and DGS techniques to allow overall size reduction exceeding 74% for the star shape slotted dualband MPA operating at 2.4 and 5 GHz frequencies. The miniaturized antenna proposed in this paper achieves wide bandwidth with measured FBWs of 38% and 13% for the two resonant frequencies, respectively, while ensuring appropriate positive gain and good efficiencies which are 2.45 dBi, 83% and 4.27 dBi, 68% at 2.4 GHz and 5 GHz, respectively.

Important miniaturization rate is attained while preserving suitable performances of the proposed antenna for WLAN-IEEE-802.11 and ISM bands in terms of gain, efficiencies, and bandwidth, proving thereby interest of high permittivity substrate technique for MPA miniaturization.

Frequency and/or polarization reconfigurability of the compact antenna will be the aim of future work.

ACKNOWLEDGMENT

The authors would like to gratefully acknowledge Prof. S. M. MERIAH from Telecommunications Laboratory (LTT), University of Tlemcen and Prof. M. FEHAM from Systems and Technology of Information and Communication (STIC) University of Tlemcen, for their technical support in fabricating prototypes of antennas and providing the experimental data.

REFERENCES

1. Rothwell, E. J. and R. O. Ouedraogo, "Antenna miniaturization: Definitions, concepts, and a review with emphasis on metamaterials," *Journal of Electromagnetic Waves and Applications*, Vol. 28, No. 17, 2089–2123, Nov. 2014, doi: 10.1080/09205071.2014.972470.
2. Fallahpour, M. and R. Zoughi, "Antenna miniaturization techniques: A review of topology- and material-based methods," *IEEE Antennas Propag. Mag.*, Vol. 60, No. 1, 38–50, Feb. 2018, doi: 10.1109/MAP.2017.2774138.
3. Lee, B. and F. J. Harackiewicz, "Miniature microstrip antenna with a partially filled high-permittivity substrate," *IEEE Trans. Antennas Propag.*, Vol. 50, No. 8, 1160–1162, Aug. 2002, doi: 10.1109/TAP.2002.801360.
4. Kula, J., D. Psychoudakis, W.-J. Liao, C.-C. Chen, J. Volakis, and J. Halloran, "Patch-antenna miniaturization using recently available ceramic substrates," *IEEE Antennas Propag. Mag.*, Vol. 48, No. 6, 13–20, Dec. 2006, doi: 10.1109/MAP.2006.323335.
5. Ullah, M. H., M. T. Islam, and J. S. Mandeep, "A parametric study of high dielectric material substrate for small antenna design," *Int. J. Appl. Electromagn. Mech.*, Vol. 41, No. 2, 193–198, Feb. 2013, doi: 10.3233/JAE-2012-1603.
6. Liu, H., S. Ishikawa, A. An, S. Kurachi, and T. Yoshimasu, "Miniaturized microstrip meander-line antenna with very high-permittivity substrate for sensor applications," *Microw. Opt. Technol. Lett.*, Vol. 49, No. 10, 2438–2440, Oct. 2007, doi: 10.1002/mop.22798.
7. Takigawa, Y., S. Kashihara, and F. Kuroki, "Integrated slot spiral antenna etched on heavily-high permittivity piece," *2007 Asia-Pacific Microwave Conference*, 1–4, Bangkok, Thailand, 2007, doi: 10.1109/APMC.2007.4554932.
8. Bhadouria, A. S. and M. Kumar, "Microstrip patch antenna for radiolocation using DGS with improved gain and bandwidth," *2014 International Conference on Advances in Engineering & Technology Research (ICAETR — 2014)*, 1–5, Unnao, India, 2014, doi: 10.1109/ICAETR.2014.7012873.

9. Pasha, M. I., C. Kumar, and D. Guha, "Simultaneous compensation of microstrip feed and patch by defected ground structure for reduced cross-polarized radiation," *IEEE Trans. Antennas Propag.*, Vol. 66, No. 12, 7348–7352, Dec. 2018, doi: 10.1109/TAP.2018.2869252.
10. Kumar, C., M. I. Pasha, and D. Guha, "Microstrip patch with nonproximal symmetric defected ground structure (DGS) for improved cross-polarization properties over principal radiation planes," *IEEE Antennas Wirel. Propag. Lett.*, Vol. 14, 1412–1414, 2015, doi: 10.1109/LAWP.2015.2406772.
11. Rahman, M. M., M. S. Islam, H. Y. Wong, T. Alam, and M. T. Islam, "Performance analysis of a defected ground-structured antenna loaded with stub-slot for 5G communication," *Sensors*, Vol. 19, No. 11, 2634, Jun. 2019, doi: 10.3390/s19112634.
12. Reddy, B. R. S. and D. Vakula, "Compact Zigzag-shaped-slit microstrip antenna with circular defected ground structure for wireless applications," *IEEE Antennas Wirel. Propag. Lett.*, Vol. 14, 678–681, 2015, doi: 10.1109/LAWP.2014.2376984.
13. Christodoulou, C. G., Y. Tawk, S. A. Lane, and S. R. Erwin, "Reconfigurable antennas for wireless and space applications," *Proc. IEEE*, Vol. 100, No. 7, 2250–2261, Jul. 2012, doi: 10.1109/JPROC.2012.2188249.
14. Su, H., H. Hu, B. Shu, B. Wang, W. Wang, and J. Wang, "Research of the SPiN diodes for silicon-based reconfigurable holographic antenna," *Solid-State Electron.*, Vol. 146, 28–33, Aug. 2018, doi: 10.1016/j.sse.2018.05.001.
15. Majid, H. A., M. K. A. Rahim, M. R. Hamid, M. F. Ismail, and F. Malek, "Frequency reconfigurable wide to narrow band monopole with slotted ground plane antenna," *Journal of Electromagnetic Waves and Applications*, Vol. 26, No. 11–12, 1460–1469, Aug. 2012, doi: 10.1080/09205071.2012.702536.
16. Salim, M. and A. Pourziad, "A novel reconfigurable spiral-shaped monopole antenna for biomedical applications," *Progress In Electromagnetics Research Letters*, Vol. 57, 79–84, 2015.
17. Ferouani, S. S., Z. Z. Bendahmane, and A. A. T. Ahmed, "Design and analysis of dual band star shape slotted patch antenna," *Microw. Rev.*, Vol. 23, No. 1, 5, 2017.
18. Laheurte, J.-M. (ed.), *Compact Antennas for Wireless Communications and Terminals: Theory and Design*, John Wiley & Sons, Inc., Hoboken, NJ, USA, 2011.
19. Salih, A. A. and M. S. Sharawi, "A dual-band highly miniaturized patch antenna," *IEEE Antennas Wirel. Propag. Lett.*, Vol. 15, 1783–1786, 2016, doi: 10.1109/LAWP.2016.2536678.
20. Jafargholi, A., A. Jafargholi, and B. Ghalamkari, "Dual-band slim microstrip patch antennas," *IEEE Trans. Antennas Propag.*, Vol. 66, No. 12, 6818–6825, Dec. 2018, doi: 10.1109/TAP.2018.2871964.
21. Roy, S. and U. Chakraborty, "Metamaterial-embedded dual wideband microstrip antenna for 2.4 GHz WLAN and 8.2 GHz ITU band applications," *Waves Random Complex Media*, 1–15, Jul. 2018, doi: 10.1080/17455030.2018.1494396.
22. Anantha, B. and R. S. R. Gosula, "Compact single feed dual band microstrip patch antenna with adjustable dual circular polarization," *IETE J. Res.*, 1–9, Apr. 2019, doi: 10.1080/03772063.2019.1598293.
23. Patel, R. H. and T. K. Upadhyaya, "Compact planar dual band antenna for WLAN application," *Progress In Electromagnetics Research Letters*, Vol. 70, 89–97, 2017.
24. Kukreja, J., D. Kumar Choudhary, and R. Kumar Chaudhary, "CPW fed miniaturized dual-band short-ended metamaterial antenna using modified split-ring resonator for wireless application," *Int. J. RF Microw. Comput.-Aided Eng.*, Vol. 27, No. 8, e21123, Oct. 2017, doi: 10.1002/mmce.21123.
25. Gupta, A. and R. K. Chaudhary, "The metamaterial antenna: A novel miniaturized dual-band coplanar waveguide-fed antenna with backed ground plane," *IEEE Antennas Propag. Mag.*, Vol. 60, No. 4, 41–48, Aug. 2018, doi: 10.1109/MAP.2018.2839894.